Springer

Journal of
Mechanical
Science and
Technology

Journal of Mechanical Science and Technology 22 (2008) 203~212

www.springerlink.com/content/1738-494x

Sub-domain reduction method in non-matched interface problems

Hyungi Kim and Maenghyo Cho*

School of Mechanical and Aerospace Engineering, Seoul National Univ., San 56-1, Shillim-dong, Kwanak-gu, Seoul, 151-742, Korea

(Manuscript Received September 5, 2006; Revised July 19, 2007; Accepted August 27, 2007)

Abstract

A sub-domain scheme combined with a reduced system is proposed for non-matched interface problems. A two-level condensation scheme (TLCS) is employed for the selection of primary degrees of freedom of each sub-domain. The degrees of freedom of each domain are divided into primary, secondary and interface degrees of freedom. After the reduced system is constructed in subdomain-level, the penalty frame method, which utilizes a conventional FEM solver, is employed for assembling non-matched subdomains. The present method can construct the reduced system of each domain without coupling with adjacent subdomains. Thus it is remarkably efficient in computation time and does not require a full memory of global system. Numerical examples demonstrate that the proposed method saves computational cost effectively and provides a reduced system which predicts the accurate eigenvalues of global system.

Keywords: Two-level condensation scheme; Sub-domain method; Reduction method; Penalty frame method

1. Introduction

The sub-domain method has been widely applied for the analysis of large-scaled structures in the automobile and aircraft industries. This method is based on partitioning the original structure into a number of subsystems. It is quite useful for specialized fields in which many substructures need to be analyzed independently [1-3]. After construction of each sub-domain, all interfaces nodes should be attached to satisfy conformity condition for global analysis. But, there may exist interface domains with non-matched mesh bet-ween sub-domains. For resolving this non-matched interface problem, a hybrid interface method with Lagrange multipliers has been proposed [4]. Previous researches have reported that this hybrid interface method provides a reliable solution to the internal fluid-structure interaction problem, coupling analysis with non-conforming sub-systems or assembled analysis of different types of elements. Besides this method, the mortar method, which does not require compatibility on the boundary interface between sub-domains, has been employed for solving non-matched problems [5]. But because these methods do not construct symmetric systems, special solvers such as the frontal solver should be employed to perform global analysis instead of a general FEM solver such as banded solver or skyline solver.

This study focuses on the development of a combined methodology between reduction scheme and sub-domain method with non-matched interface. Moreover, the methodology of the present method can be applied for wide structural analysis such as dynamic problems or time integration regardless of the kind of interface scheme. So, we employ the penalty frame method, which is easy to implement. The penalty frame method was proposed by Cho and Kim in order to connect the incompatible interface mesh between non-matched sub-domains [6] The determination of proper penalty parameter values was reported by Pantano and Averill [7, 8].

*Corresponding author. Tel.: +82 2 880 1693, Fax.: +82 2 886 1693
E-mail address: mhcho@snu.ac.kr
DOI 10.1007/s12206-007-1033-6

In this method, because the function of the continuity constraint is evaluated with quadratic form, it constructs a symmetric matrix which utilizes a common FEM solver.

In first step of the present method, reduced systems based on PDOFs are constructed in each sub-domain. For a reliable selection of PDOFs of each domain, a two-level condensation scheme (TLCS) of PDOFs is employed [9-11]. The detail description related to this step is given in the reference by Cho and Kim. Then, in the second step, each reduced system is assembled by penalty frame of each domain interface.

The construction of the each reduced system does not take much time because the reduced system is just constructed in each subdomain-level, not in the global domain level. Moreover, this scheme does not need full memory storage for the global system, but just requires the size of each sub-domain system. After the selection of PDOFs in each domain, IRS is employed to construct the final reduced system. Although there are several reduction schemes to improve the results, IRS is adequate to obtain reliable results, as shown in Kim and Cho [12].

In the numerical examples of non-matched systems, the efficiency and reliability of the proposed scheme are verified through an eigenvalue analysis. The key issue of this paper is on how to select PDOFs among all the active DOFs at sub-domain level and assemble each domain with interface attaching scheme effectively. This can be achieved by constructing the reduced system based on IRS and assembling each reduced system from a multi-domain structure.

2. Sub-domain method combined with reduced system in non-matched problem

The reduction scheme is very efficient for large-scale problems. Once the reduced system is well-constructed, it can be applied to various kinds of problems with saving the computer resource and time cost. But, in a problem with several hundred thousand DOFs, the single domain reduction scheme has a limitation in selecting PDOFs. This situation can be improved by combining with reduction method and sub-domain scheme. But, in a non-matched interface problem, the continuity condition of the attached interfaces should be considered in the reduction scheme, which was not considered in the matched interface problem.

In this section, we evaluate the continuity conditions through penalty frame method, and provide the reduction system of a non-matched interface problem.

2.1 Continuity condition of non-matched interface

We often encounter a problem with several subdomains which are constructed independently. In this case, the interface nodes of each system are not matched to one another. Although the hybrid interface method, which employs Lagrange multipliers, is popular, the present study employs the penalty function method to apply displacement continuity constraints because of its simplicity and the guarantee of symmetric banded nature of global stiffness matrix.

To perform a coupled analysis of assemblage of the subdomains with the non-matched interfaces, the virtual frame displacement $\mathbf{v}_b$ is required for the assemblage of each sub-system. Fig. 1 shows the plate structure with non-matched sub-domain interfaces. To impose the continuity condition between sub-domain 1 and sub-domain 2, a penalty frame method is introduced. The variational statement for continuity condition between each sub-domain is given in Eq. (1). Here, $\mathbf{u}_b^{(1)}$ and $\mathbf{u}_b^{(2)}$ are the penalty frame displacement field of each sub-domain, respectively.

$$\begin{aligned}
\Pi_{S_v} &= \frac{k}{2}\int_{S_1}\left(\mathbf{u}_b^{(1)}-\mathbf{v}_b\right)^2 ds + \frac{k}{2}\int_{S_2}\left(\mathbf{u}_b^{(2)}-\mathbf{v}_b\right)^2 ds \\
\delta\Pi_{S_v} &= k\int_{S_1}\left(\mathbf{u}_b^{(1)}-\mathbf{v}_b\right)\left(\delta\mathbf{u}_b^{(1)}-\delta\mathbf{v}_b\right)ds \\
&\quad + k\int_{S_2}\left(\mathbf{u}_b^{(2)}-\mathbf{v}_b\right)\left(\delta\mathbf{u}_b^{(2)}-\delta\mathbf{v}_b\right)ds
\end{aligned} \tag{1}$$

A piecewise linear function is used for the shape functions of $\mathbf{u}_b^{(1)},\mathbf{u}_b^{(2)},\mathbf{v}_b$. The shape functions for $\mathbf{u}_b^{(1)},\mathbf{u}_b^{(2)}$ and $\mathbf{v}_b$ are expressed as $\mathbf{N}_i, \mathbf{N}_j$ and $\mathbf{T}_b$.

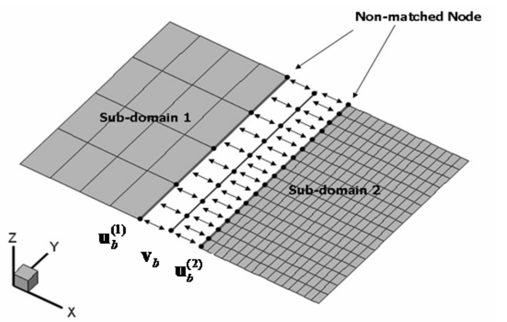

Fig. 1. Assemblage of non-matched systems by virtual interface frame.

Eq. (2) is obtained from Eq. (1) by substituting shape functions.

$$
\begin{aligned}
\boldsymbol{\delta\pi} &= k_1 \int_{s_1} \left(\mathbf{N}_i \mathbf{u}_b^{(1)} - \mathbf{T}_b \mathbf{v}_b\right)\left(\mathbf{N}_i \boldsymbol{\delta}\mathbf{u}_b^{(1)} - \mathbf{T}_b \boldsymbol{\delta}\mathbf{v}_b\right) ds \\
&\quad + k_2 \int_{s_2} \left(\mathbf{N}_j \mathbf{u}_b^{(2)} - \mathbf{T}_b \mathbf{v}_b\right)\left(\mathbf{N}_j \boldsymbol{\delta}\mathbf{u}_b^{(2)} - \mathbf{T}_b \boldsymbol{\delta}\mathbf{v}_b\right) ds \\
&= k_1 \int_{s_1} \left(\mathbf{N}_i^{\mathbf{T}} \mathbf{N}_i \mathbf{u}_b^{(1)} - \mathbf{N}_i^{\mathbf{T}} \mathbf{T}_b \mathbf{v}_b\right) \boldsymbol{\delta}\mathbf{u}_i ds \\
&\quad + k_1 \int_{s_1} \left(\mathbf{T}_b^{\mathbf{T}} \mathbf{T}_b \mathbf{v}_b - \mathbf{N}_i^{\mathbf{T}} \mathbf{T}_b \mathbf{u}_b^{(1)}\right) \boldsymbol{\delta}\mathbf{v}_b ds \\
&\quad + k_2 \int_{s_2} \left(\mathbf{N}_j^{\mathbf{T}} \mathbf{N}_j \mathbf{u}_b^{(2)} - \mathbf{N}_j^{\mathbf{T}} \mathbf{T}_b \mathbf{v}_b\right) \boldsymbol{\delta}\mathbf{u}_j ds \\
&\quad + k_2 \int_{s_2} \left(\mathbf{T}_b^{\mathbf{T}} \mathbf{T}_b \mathbf{v}_b - \mathbf{N}_j^{\mathbf{T}} \mathbf{T}_b \mathbf{u}_b^{(2)}\right) \boldsymbol{\delta}\mathbf{v}_b ds = 0
\end{aligned}
$$

$$
\therefore \begin{cases}
\boldsymbol{\delta}\mathbf{u}_b^{(1)} : k_1 \int_{s_1} \left(\mathbf{N}_i^{\mathbf{T}} \mathbf{N}_i \mathbf{u}_b^{(1)} - \mathbf{N}_i^{\mathbf{T}} \mathbf{T}_b \mathbf{v}_b\right) ds = 0, \\
\boldsymbol{\delta}\mathbf{v}_b^{1} : k_1 \int_{s_1} \left(\mathbf{T}_b^{\mathbf{T}} \mathbf{T}_b \mathbf{v}_b - \mathbf{N}_i^{\mathbf{T}} \mathbf{T}_b \mathbf{u}_b\right) ds = 0 \\
\boldsymbol{\delta}\mathbf{u}_b^{(2)} : k_2 \int_{s_2} \left(\mathbf{N}_j^{\mathbf{T}} \mathbf{N}_j \mathbf{u}_b^{(2)} - \mathbf{N}_j^{\mathbf{T}} \mathbf{T}_b \mathbf{v}_b\right) ds = 0, \\
\boldsymbol{\delta}\mathbf{v}_b^{2} : k_2 \int_{s_2} \left(\mathbf{T}_b^{\mathbf{T}} \mathbf{T}_b \mathbf{v}_b - \mathbf{N}_j^{\mathbf{T}} \mathbf{T}_b \mathbf{u}_b^{(2)}\right) ds = 0
\end{cases} \tag{2}
$$

Where,

$$
\begin{aligned}
&\mathbf{g}_{ii}^{(1)} = k_1 \int_{s_1} \mathbf{N}_i^{\mathbf{T}} \mathbf{N}_i ds, \quad \mathbf{g}_{ib}^{(1)} = -k_1 \int_{s_1} \mathbf{N}_i^{\mathbf{T}} \mathbf{T}_b ds, \\
&\mathbf{g}_{bi}^{(1)} = -k_1 \int_{s_1} \mathbf{N}_i^{\mathbf{T}} \mathbf{T}_b ds, \ \mathbf{g}_{bb}^{(1)} = k_1 \int_{s_1} \mathbf{T}_b^{\mathbf{T}} \mathbf{T}_b ds \\
&\mathbf{g}_{jj}^{(2)} = k_2 \int_{s_2} \mathbf{N}_j^{\mathbf{T}} \mathbf{N}_j ds, \ \mathbf{g}_{jb}^{(2)} = -k_2 \int_{s_2} \mathbf{N}_j^{\mathbf{T}} \mathbf{T}_b ds, \\
&\mathbf{g}_{bj}^{(2)} = -k_2 \int_{s_2} \mathbf{N}_j^{\mathbf{T}} \mathbf{T}_b ds, \ \mathbf{g}_{bb}^{(2)} = k_2 \int_{s_2} \mathbf{T}_b^{\mathbf{T}} \mathbf{T}_b ds
\end{aligned}
$$

2.2 Formulation of reduced system considering the penalty interface frame

Interface functional of Eq. (2) is expressed in the following matrix form as shown in Eq. (3). Numbers (1) and (2) in superscript symbol indicates the sub-domain (1) and (2).

$$
\begin{bmatrix}
\mathbf{g}_{ii}^{(1)} & \mathbf{g}_{ib}^{(1)} & 0 \\
\mathbf{g}_{bi}^{(1)} & \mathbf{g}_{bb} & \mathbf{g}_{bj}^{(2)} \\
0 & \mathbf{g}_{jb}^{(2)} & \mathbf{g}_{jj}^{(2)}
\end{bmatrix}
\begin{bmatrix}
\mathbf{u}_b^{(1)} \\ \mathbf{v}_b \\ \mathbf{u}_b^{(2)}
\end{bmatrix}, \quad \mathbf{g}_{bb} = \mathbf{g}_{bb}^{(1)} + \mathbf{g}_{bb}^{(2)} \tag{3}
$$

Considering the interface matrix in Eq. (3), the global matrix of the non-matched system is constructed as follows:

$$
\begin{bmatrix}
\mathbf{K}_{pp}^{(1)} & \mathbf{K}_{ps}^{(1)} & \mathbf{K}_{pb}^{(1)} & 0 & 0 & 0 & 0 \\
\mathbf{K}_{sp}^{(1)} & \mathbf{K}_{ss}^{(1)} & \mathbf{K}_{sb}^{(1)} & 0 & 0 & 0 & 0 \\
\mathbf{K}_{bp}^{(1)} & \mathbf{K}_{bs}^{(1)} & \left(\mathbf{K}_{bb}^{(1)} + \mathbf{g}_{ii}^{(1)}\right) & \mathbf{g}_{ib}^{(1)} & 0 & 0 & 0 \\
0 & 0 & \mathbf{g}_{bi}^{(1)} & \mathbf{g}_{bb} & \mathbf{g}_{bj}^{(2)} & 0 & 0 \\
0 & 0 & 0 & \mathbf{g}_{jb}^{(2)} & \left(\mathbf{K}_{bb}^{(2)} + \mathbf{g}_{jj}^{(2)}\right) & \mathbf{K}_{bs}^{(2)} & \mathbf{K}_{bp}^{(2)} \\
0 & 0 & 0 & 0 & \mathbf{K}_{sb}^{(2)} & \mathbf{K}_{ss}^{(2)} & \mathbf{K}_{sp}^{(2)} \\
0 & 0 & 0 & 0 & \mathbf{K}_{pb}^{(2)} & \mathbf{K}_{ps}^{(2)} & \mathbf{K}_{pp}^{(2)}
\end{bmatrix}
\begin{Bmatrix}
\mathbf{u_p}^{(1)} \\ \mathbf{u_s}^{(1)} \\ \mathbf{u_b}^{(1)} \\ \mathbf{v}_b \\ \mathbf{u_b}^{(2)} \\ \mathbf{u_s}^{(2)} \\ \mathbf{u_p}^{(2)}
\end{Bmatrix}
= \boldsymbol{\lambda}
\begin{bmatrix}
\mathbf{M}_{pp}^{(1)} & \mathbf{M}_{ps}^{(1)} & \mathbf{M}_{pb}^{(1)} & 0 & 0 & 0 & 0 \\
\mathbf{M}_{sp}^{(1)} & \mathbf{M}_{ss}^{(1)} & \mathbf{M}_{sb}^{(1)} & 0 & 0 & 0 & 0 \\
\mathbf{M}_{bp}^{(1)} & \mathbf{M}_{bs}^{(1)} & \mathbf{M}_{bb}^{(1)} & 0 & 0 & 0 & 0 \\
0 & 0 & 0 & 0 & 0 & 0 & 0 \\
0 & 0 & 0 & 0 & \mathbf{M}_{bb}^{(2)} & \mathbf{M}_{bs}^{(2)} & \mathbf{M}_{bp}^{(2)} \\
0 & 0 & 0 & 0 & \mathbf{M}_{sb}^{(2)} & \mathbf{M}_{ss}^{(2)} & \mathbf{M}_{sp}^{(2)} \\
0 & 0 & 0 & 0 & \mathbf{M}_{pb}^{(2)} & \mathbf{M}_{ps}^{(2)} & \mathbf{M}_{pp}^{(2)}
\end{bmatrix}
\begin{Bmatrix}
\mathbf{u_p}^{(1)} \\ \mathbf{u_s}^{(1)} \\ \mathbf{u_b}^{(1)} \\ \mathbf{v}_b \\ \mathbf{u_b}^{(2)} \\ \mathbf{u_s}^{(2)} \\ \mathbf{u_p}^{(2)}
\end{Bmatrix} \tag{4}
$$

where, the subscript symbols ***p***, ***s*** and ***b*** represent the primary degrees of freedom (PDOF), the secondary degrees of freedom (SDOF), and the interface degrees of freedom (IDOF), respectively.

For the construction of the reduced system, SDOFs of domain 1 and domain 2 are eliminated from Eq. (4). The related equations obtained from the second and sixth rows of Eq. (4) are given in Eq. (5).

$$
\begin{aligned}
&\mathbf{K}_{sp}^{(1)} \mathbf{u}_p^{(1)} + \mathbf{K}_{ss}^{(1)} \mathbf{u}_s^{(1)} + \mathbf{K}_{sb}^{(1)} \mathbf{u}_b^{(1)} \\
&\quad = \boldsymbol{\lambda}\left(\mathbf{M}_{sp}^{(1)} \mathbf{u}_p^{(1)} + \mathbf{M}_{ss}^{(1)} \mathbf{u}_s^{(1)} + \mathbf{M}_{sb}^{(1)} \mathbf{u}_b^{(1)}\right) \\
&\mathbf{K}_{sb}^{(2)} \mathbf{u}_b^{(2)} + \mathbf{K}_{ss}^{(2)} \mathbf{u}_s^{(2)} + \mathbf{K}_{sp}^{(2)} \mathbf{u}_p^{(2)} \\
&\quad = \boldsymbol{\lambda}\left(\mathbf{M}_{sb}^{(2)} \mathbf{u}_b^{(2)} + \mathbf{M}_{ss}^{(2)} \mathbf{u}_s^{(2)} + \mathbf{M}_{sp}^{(2)} \mathbf{u}_p^{(2)}\right)
\end{aligned} \tag{5}
$$

Additionally, a non-matched system requires a third transformation equation related to the interface frame. This relation is obtained from the fourth row of Eq. (4) as shown in Eq. (6).

$$
\mathbf{v}_b = -\mathbf{g}_{bb}^{-1}\left(\mathbf{g}_{bi}^{(1)} \mathbf{u}_b^{(1)} + \mathbf{g}_{bj}^{(2)} \mathbf{u}_b^{(2)}\right) \tag{6}
$$

where, $\mathbf{G}^{(1)} = -\mathbf{g}_{bb}^{-1} \mathbf{g}_{bi}^{(1)}$, $\mathbf{G}^{(2)} = -\mathbf{g}_{bb}^{-1} \mathbf{g}_{bj}^{(2)}$, and $\mathbf{v}_b = \mathbf{G}^{(1)} \mathbf{u}_b^{(1)} + \mathbf{G}^{(2)} \mathbf{u}_b^{(2)}$

In a non-matched system, the transformation relation of PDOFs, IDOFs and SDOFs is identical to that of the matched system as given in Kim and Cho [12].

In Eq. (5), the transformation relation between PDOFs, IDOFs and SDOFs can be obtained. From the second equation of Eq. (5), SDOFs $\mathbf{u}_s^{(1)}$ of sub-domain 1 is evaluated as Eq. (7).

$$\begin{aligned}\mathbf{u}_s^{(1)} &= -\left(\mathbf{K}_{ss}^{(1)} - \boldsymbol{\lambda}\mathbf{M}_{ss}^{(1)}\right)^{-1}\left(\mathbf{K}_{sp}^{(1)} - \boldsymbol{\lambda}\mathbf{M}_{sp}^{(1)}\right)\mathbf{u}_p^{(1)} \\ &\quad -\left(\mathbf{K}_{ss}^{(1)} - \boldsymbol{\lambda}\mathbf{M}_{ss}^{(1)}\right)^{-1}\left(\mathbf{K}_{sb}^{(1)} - \boldsymbol{\lambda}\mathbf{M}_{sb}^{(1)}\right)\mathbf{u}_b\end{aligned} \tag{7}$$

The term $\left(\mathbf{K}_{ss}^{(1)} - \boldsymbol{\lambda}\mathbf{M}_{ss}^{(1)}\right)^{-1}$ can be expanded by series expansion as follows:

$$\begin{aligned}\left(\mathbf{K}_{ss}^{(1)} - \boldsymbol{\lambda}\mathbf{M}_{ss}^{(1)}\right)^{-1} = \Big[\mathbf{I} &+ \boldsymbol{\lambda}\left(\mathbf{K}_{ss}^{(1)}\right)^{-1}\mathbf{M}_{ss}^{(1)} \\ &+ \left[\boldsymbol{\lambda}\left(\mathbf{K}_{ss}^{(1)}\right)^{-1}\mathbf{M}_{ss}^{(1)}\right]^2 \\ &+ \left[\boldsymbol{\lambda}\left(\mathbf{K}_{ss}^{(1)}\right)^{-1}\mathbf{M}_{ss}^{(1)}\right]^3 \\ &+ \mathbf{....}\Big]\left(\mathbf{K}_{ss}^{(1)}\right)^{-1}\end{aligned} \tag{8}$$

When the first-order term of $\boldsymbol{\lambda}$ is included, SDOFs can be expressed as the following one:

$$\begin{aligned}\mathbf{u}_s^{(1)} &= -\left[\mathbf{K}_{ss}^{(1)}\right]^{-1}\mathbf{K}_{sp}^{(1)}\mathbf{u}_p^{(1)} - \left[\mathbf{K}_{ss}^{(1)}\right]^{-1}\mathbf{K}_{sb}^{(1)}\mathbf{u}_b \\ &\quad + \left[\mathbf{K}_{ss}^{(1)}\right]^{-1}\left(\mathbf{M}_{sp}^{(1)} - \mathbf{M}_{ss}^{(1)}\left[\mathbf{K}_{ss}^{(1)}\right]^{-1}\mathbf{K}_{sp}^{(1)}\right)\boldsymbol{\lambda}\mathbf{u}_p^{(1)} \\ &\quad + \left[\mathbf{K}_{ss}^{(1)}\right]^{-1}\left(\mathbf{M}_{sb}^{(1)} - \mathbf{M}_{ss}^{(1)}\left[\mathbf{K}_{ss}^{(1)}\right]^{-1}\mathbf{K}_{sb}^{(1)}\right)\boldsymbol{\lambda}\mathbf{u}_b\end{aligned} \tag{9}$$

To express this equation in a compact symbolic form, the matrices $\mathbf{T}_{sp}^{(1)}$ and $\mathbf{T}_{sb}^{(1)}$ are defined as follows:

$$\mathbf{T}_{sp}^{(1)} = -\left[\mathbf{K}_{ss}^{(1)}\right]^{-1}\mathbf{K}_{sp}^{(1)},\ \mathbf{T}_{sb}^{(1)} = -\left[\mathbf{K}_{ss}^{(1)}\right]^{-1}\mathbf{K}_{sb}^{(1)} \tag{10}$$

The relation of PDOFs, SDOFs and IDOFs can be expressed in matrix form as Eq. (11).

$$\begin{bmatrix}\mathbf{u}_p^{(1)} \\ \mathbf{u}_s^{(1)} \\ \mathbf{u}_b\end{bmatrix} = \begin{bmatrix}\mathbf{I} & 0 \\ \left\{\mathbf{T}_{sp}^{(1)} + \left[\mathbf{K}_{ss}^{(1)}\right]^{-1}\left(\mathbf{M}_{sp}^{(1)} + \mathbf{M}_{ss}^{(1)}\mathbf{T}_{sp}^{(1)}\right)\boldsymbol{\lambda}\right\} & \left\{\mathbf{T}_{sb}^{(1)} + \left[\mathbf{K}_{ss}^{(1)}\right]^{-1}\left(\mathbf{M}_{sb}^{(1)} + \mathbf{M}_{ss}^{(1)}\mathbf{T}_{sb}^{(1)}\right)\boldsymbol{\lambda}\right\} \\ 0 & \mathbf{I}\end{bmatrix}\begin{bmatrix}\mathbf{u}_p^{(1)} \\ \mathbf{u}_b\end{bmatrix} = \mathbf{T}_1\begin{bmatrix}\mathbf{u}_p^{(1)} \\ \mathbf{u}_b\end{bmatrix} \tag{11}$$

Similar to the relation of sub-domain 1 of Eq. (11), the transformation relation of sub-domain 2 can be expressed as Eq. (12).

$$\begin{bmatrix}\mathbf{u}_b \\ \mathbf{u}_s^{(2)} \\ \mathbf{u}_p^{(2)}\end{bmatrix} = \begin{bmatrix}\mathbf{I} & 0 \\ \left\{\mathbf{T}_{sb}^{(2)} + \left[\mathbf{K}_{ss}^{(2)}\right]^{-1}\left(\mathbf{M}_{sb}^{(2)} + \mathbf{M}_{ss}^{(2)}\mathbf{T}_{sb}^{(2)}\right)\boldsymbol{\lambda}\right\} & \left\{\mathbf{T}_{sp}^{(2)} + \left[\mathbf{K}_{ss}^{(2)}\right]^{-1}\left(\mathbf{M}_{sp}^{(2)} + \mathbf{M}_{ss}^{(2)}\mathbf{T}_{sp}^{(2)}\right)\boldsymbol{\lambda}\right\} \\ 0 & \mathbf{I}\end{bmatrix}\begin{bmatrix}\mathbf{u}_b \\ \mathbf{u}_p^{(2)}\end{bmatrix} = \mathbf{T}_2\begin{bmatrix}\mathbf{u}_b \\ \mathbf{u}_p^{(2)}\end{bmatrix} \tag{12}$$

In the above transformation relation, the Guyan method ignores all eigenvalue terms [13]. Therefore, the Guyan method generates excessive errors in the prediction of eigenvalues except in the range of only the few lowest eigenvalues. In this study, we employ IRS, considering the first-order eigenvalue term [14]. The IRS method provides reliable results and it does not take much time in construction of the reduced system compared to the Guyan method.

In Eqs. (11) and (12), transformation matrices are divided into constant part and first-order eigenvalue part, as given in Eqs. (13a) and (13b):

$$\mathbf{T}_1 = \begin{bmatrix}\mathbf{I} & 0 & 0 \\ \mathbf{T}_{sp}^{(1)} & \mathbf{T}_{sb}^{(1)} & 0 \\ 0 & \mathbf{I} & 0\end{bmatrix} + \begin{bmatrix}0 & 0 & \\ \left[\mathbf{K}_{ss}^{(1)}\right]^{-1}\left(\mathbf{M}_{sp}^{(1)} + \mathbf{M}_{ss}^{(1)}\mathbf{T}_{sp}^{(1)}\right) & \left[\mathbf{K}_{ss}^{(1)}\right]^{-1}\left(\mathbf{M}_{sb}^{(1)} + \mathbf{M}_{ss}^{(1)}\mathbf{T}_{sb}^{(1)}\right) & 0 \\ 0 & 0 & \end{bmatrix}\boldsymbol{\lambda} \tag{13a}$$

$$\mathbf{T}_2 = \begin{bmatrix}0 & \mathbf{I} & 0 \\ 0 & \mathbf{T}_{sb}^{(2)} & \mathbf{T}_{sp}^{(2)} \\ 0 & 0 & \mathbf{I}\end{bmatrix} + \begin{bmatrix}0 & 0 & 0 \\ 0 & \left[\mathbf{K}_{ss}^{(2)}\right]^{-1}\left(\mathbf{M}_{sb}^{(2)} + \mathbf{M}_{ss}^{(2)}\mathbf{T}_{sb}^{(2)}\right) & \left[\mathbf{K}_{ss}^{(2)}\right]^{-1}\left(\mathbf{M}_{sp}^{(2)} + \mathbf{M}_{ss}^{(2)}\mathbf{T}_{sp}^{(2)}\right) \\ 0 & 0 & 0\end{bmatrix}\boldsymbol{\lambda} \tag{13b}$$

In Eqs. (13a) and (13b), the eigenvalue $\boldsymbol{\lambda}$ mainly related to the lower modes is the unknown value. So, Guyan's static condensation can be used to replace the eigenvalue $\boldsymbol{\lambda}$. In Guyan's static condensation, an eigenvalue problem can be written in terms of PDOFs and IDOFs as follows:

$$\left[\mathbf{K}_G\right]\begin{bmatrix}\mathbf{u}_p^{(1)} \\ \mathbf{u}_b \\ \mathbf{u}_p^{(2)}\end{bmatrix} = \boldsymbol{\lambda}\left[\mathbf{M}_G\right]\begin{bmatrix}\mathbf{u}_p^{(1)} \\ \mathbf{u}_b \\ \mathbf{u}_p^{(2)}\end{bmatrix} \tag{14}$$

In Eq. (14), $\boldsymbol{\lambda}\begin{bmatrix}\mathbf{u}_p^{(1)} \\ \mathbf{u}_b \\ \mathbf{u}_p^{(2)}\end{bmatrix}$ is expressed as $\left[\mathbf{M}_G\right]^{-1}\left[\mathbf{K}_G\right]$

$$\begin{bmatrix} \mathbf{u}_p^{(1)} \\ \mathbf{u}_b \\ \mathbf{u}_p^{(2)} \end{bmatrix}.$$

Equation (15) shows the transformation relations between PDOFs, SDOFs and IDOFs in each sub-domain.

$$\underline{\text{sub-domain 1}}$$

$$\begin{bmatrix} \mathbf{u}_p^{(1)} \\ \mathbf{u}_s^{(1)} \\ \mathbf{u}_b^{(1)} \end{bmatrix} = \begin{bmatrix} \mathbf{I} & 0 \\ \mathbf{T}_{IRS}^{sp(1)} & \mathbf{T}_{IRS}^{sb(1)} \\ 0 & \mathbf{I} \end{bmatrix} \begin{bmatrix} \mathbf{u}_p^{(1)} \\ \mathbf{u}_b^{(1)} \end{bmatrix} = \mathbf{T}_1 \begin{bmatrix} \mathbf{u}_p^{(1)} \\ \mathbf{u}_b^{(1)} \end{bmatrix}$$

$$\underline{\text{virtual interface frame}}$$

$$[\mathbf{v}_b] = \begin{bmatrix} \mathbf{G}^{(1)} & \mathbf{G}^{(2)} \end{bmatrix} \begin{bmatrix} \mathbf{u}_b^{(1)} \\ \mathbf{u}_b^{(2)} \end{bmatrix} = \mathbf{T}_v \begin{bmatrix} \mathbf{u}_b^{(1)} \\ \mathbf{u}_b^{(2)} \end{bmatrix} \tag{15}$$

$$\underline{\text{sub-domain 2}}$$

$$\begin{bmatrix} \mathbf{u}_b^{(2)} \\ \mathbf{u}_s^{(2)} \\ \mathbf{u}_p^{(2)} \end{bmatrix} = \begin{bmatrix} \mathbf{I} & 0 \\ \mathbf{T}_{IRS}^{sb(2)} & \mathbf{T}_{IRS}^{sp(2)} \\ 0 & \mathbf{I} \end{bmatrix} \begin{bmatrix} \mathbf{u}_b^{(2)} \\ \mathbf{u}_p^{(2)} \end{bmatrix} = \mathbf{T}_2 \begin{bmatrix} \mathbf{u}_b^{(2)} \\ \mathbf{u}_p^{(2)} \end{bmatrix}$$

$$\mathbf{T}_{IRS}^{sp(1)} = \mathbf{T}_{sp}^{(1)} + \left[\mathbf{K}_{ss}^{(1)}\right]^{-1}\left(\mathbf{M}_{sp}^{(1)} + \mathbf{M}_{ss}^{(1)}\mathbf{T}_{sp}^{(1)}\right)\boldsymbol{\lambda},\ \mathbf{T}_{IRS}^{sb(1)} = \mathbf{T}_{sb}^{(1)} + \left[\mathbf{K}_{ss}^{(1)}\right]^{-1}\left(\mathbf{M}_{sb}^{(1)} + \mathbf{M}_{ss}^{(1)}\mathbf{T}_{sb}^{(1)}\right)\boldsymbol{\lambda}$$

$$\mathbf{T}_{IRS}^{sb(2)} = \mathbf{T}_{sb}^{(2)} + \left[\mathbf{K}_{ss}^{(2)}\right]^{-1}\left(\mathbf{M}_{sb}^{(2)} + \mathbf{M}_{ss}^{(2)}\mathbf{T}_{sb}^{(2)}\right)\boldsymbol{\lambda},\ \mathbf{T}_{IRS}^{sp(2)} = \mathbf{T}_{sp}^{(2)} + \left[\mathbf{K}_{ss}^{(2)}\right]^{-1}\left(\mathbf{M}_{sp}^{(2)} + \mathbf{M}_{ss}^{(2)}\mathbf{T}_{sp}^{(2)}\right)\boldsymbol{\lambda}$$

From using the transformation relation of Eq. (15), the final reduced stiffness, mass and interface matrices of non-matched two field systems are obtained as Eqs. (16) and (17), respectively. Fig. 2 shows the assembled configuration of the stiffness and mass matrix in the non-matched interface system.

$$\mathbf{K}_{IRS}^{1} = \begin{bmatrix} \mathbf{I} & \mathbf{T}_{IRS}^{sp(1)} & 0 \\ 0 & \mathbf{T}_{IRS}^{sb(1)} & \mathbf{I} \end{bmatrix} \begin{bmatrix} \mathbf{K}_{pp}^{(1)} & \mathbf{K}_{ps}^{(1)} & \mathbf{K}_{pb}^{(1)} \\ \mathbf{K}_{sp}^{(1)} & \mathbf{K}_{ss}^{(1)} & \mathbf{K}_{sb}^{(1)} \\ \mathbf{K}_{bp}^{(1)} & \mathbf{K}_{bs}^{(1)} & \left(\mathbf{K}_{bb}^{(1)} + \mathbf{g}_{ii}^{(1)}\right) \end{bmatrix} \begin{bmatrix} \mathbf{I} & 0 \\ \mathbf{T}_{IRS}^{sp(1)} & \mathbf{T}_{IRS}^{sb(1)} \\ 0 & \mathbf{I} \end{bmatrix}$$

$$\mathbf{K}_{IRS}^{2} = \begin{bmatrix} \mathbf{I} & \mathbf{T}_{IRS}^{sb(2)} & 0 \\ 0 & \mathbf{T}_{IRS}^{sp(2)} & \mathbf{I} \end{bmatrix} \begin{bmatrix} \left(\mathbf{K}_{bb}^{(2)} + \mathbf{g}_{jj}^{(2)}\right) & \mathbf{K}_{bs}^{(2)} & \mathbf{K}_{bp}^{(2)} \\ \mathbf{K}_{sb}^{(2)} & \mathbf{K}_{ss}^{(2)} & \mathbf{K}_{sp}^{(2)} \\ \mathbf{K}_{pb}^{(2)} & \mathbf{K}_{ps}^{(2)} & \mathbf{K}_{pp}^{(2)} \end{bmatrix} \begin{bmatrix} \mathbf{I} & 0 \\ \mathbf{T}_{IRS}^{sb(2)} & \mathbf{T}_{IRS}^{sp(2)} \\ 0 & \mathbf{I} \end{bmatrix}$$

$$\mathbf{K}_{IRS}^{v} = \begin{bmatrix} \mathbf{I} & \mathbf{G}^{(1)} & 0 \\ 0 & \mathbf{G}^{(2)} & \mathbf{I} \end{bmatrix} \begin{bmatrix} 0 & \mathbf{g}_{ib}^{(1)} & 0 \\ \mathbf{g}_{bi}^{(1)} & \mathbf{g}_{bb} & \mathbf{g}_{bj}^{(2)} \\ 0 & \mathbf{g}_{jb}^{(2)} & 0 \end{bmatrix} \begin{bmatrix} \mathbf{I} & 0 \\ \mathbf{G}^{(1)} & \mathbf{G}^{(2)} \\ 0 & \mathbf{I} \end{bmatrix} \tag{16}$$

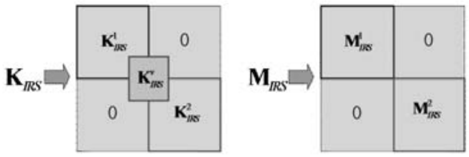

Fig. 2. Assembled configuration of the reduced stiffness and mass matrices in non-matched system.

$$\mathbf{M}_{IRS}^{1} = \begin{bmatrix} \mathbf{I} & \mathbf{T}_{IRS}^{sp(1)} & 0 \\ 0 & \mathbf{T}_{IRS}^{sb(1)} & \mathbf{I} \end{bmatrix} \begin{bmatrix} \mathbf{M}_{pp}^{(1)} & \mathbf{M}_{ps}^{(1)} & \mathbf{M}_{pb}^{(1)} \\ \mathbf{M}_{sp}^{(1)} & \mathbf{M}_{ss}^{(1)} & \mathbf{M}_{sb}^{(1)} \\ \mathbf{M}_{bp}^{(1)} & \mathbf{M}_{bs}^{(1)} & \mathbf{M}_{bb}^{(1)} \end{bmatrix} \begin{bmatrix} \mathbf{I} & 0 \\ \mathbf{T}_{IRS}^{sp(1)} & \mathbf{T}_{IRS}^{sb(1)} \\ 0 & \mathbf{I} \end{bmatrix}$$

$$\mathbf{M}_{IRS}^{2} = \begin{bmatrix} \mathbf{I} & \mathbf{T}_{IRS}^{sb(2)} & 0 \\ 0 & \mathbf{T}_{IRS}^{sp(2)} & \mathbf{I} \end{bmatrix} \begin{bmatrix} \mathbf{M}_{bb}^{(2)} & \mathbf{M}_{bs}^{(2)} & \mathbf{M}_{bp}^{(2)} \\ \mathbf{M}_{sb}^{(2)} & \mathbf{M}_{ss}^{(2)} & \mathbf{M}_{sp}^{(2)} \\ \mathbf{M}_{pb}^{(2)} & \mathbf{M}_{ps}^{(2)} & \mathbf{M}_{pp}^{(2)} \end{bmatrix} \begin{bmatrix} \mathbf{I} & 0 \\ \mathbf{T}_{IRS}^{sb(2)} & \mathbf{T}_{IRS}^{sp(2)} \\ 0 & \mathbf{I} \end{bmatrix} \tag{17}$$

Using simplified symbolic notation for $\mathbf{M}_{IRS}$ and $\mathbf{K}_{IRS}$, the final system can be given as Eq. (18):

$$\begin{bmatrix} \mathbf{K}_{IRS}^{(11)} & \mathbf{K}_{IRS}^{(12)} & 0 & 0 \\ \mathbf{K}_{IRS}^{(21)} & \mathbf{K}_{IRS}^{(22)} & \mathbf{K}_{IRS}^{(23)} & 0 \\ 0 & \mathbf{K}_{IRS}^{(32)} & \mathbf{K}_{IRS}^{(33)} & \mathbf{K}_{IRS}^{(34)} \\ 0 & 0 & \mathbf{K}_{IRS}^{(43)} & \mathbf{K}_{IRS}^{(44)} \end{bmatrix} \begin{bmatrix} \mathbf{u}_p^{(1)} \\ \mathbf{u}_b^{(1)} \\ \mathbf{u}_b^{(2)} \\ \mathbf{u}_p^{(2)} \end{bmatrix} = \boldsymbol{\lambda} \begin{bmatrix} \mathbf{M}_{IRS}^{(11)} & \mathbf{M}_{IRS}^{(12)} & 0 & 0 \\ \mathbf{M}_{IRS}^{(21)} & \mathbf{M}_{IRS}^{(22)} & \mathbf{M}_{IRS}^{(23)} & 0 \\ 0 & \mathbf{M}_{IRS}^{(32)} & \mathbf{M}_{IRS}^{(33)} & \mathbf{M}_{IRS}^{(34)} \\ 0 & 0 & \mathbf{M}_{IRS}^{(43)} & \mathbf{M}_{IRS}^{(44)} \end{bmatrix} \begin{bmatrix} \mathbf{u}_p^{(1)} \\ \mathbf{u}_b^{(1)} \\ \mathbf{u}_b^{(2)} \\ \mathbf{u}_p^{(2)} \end{bmatrix} \tag{18}$$

Each component of the reduced stiffness and mass matrices is given in the following expressions:

$$\mathbf{K}_{IRS}^{(11)} = \mathbf{K}_{pp}^{(1)} + \mathbf{K}_{ps}^{(1)}\mathbf{T}_{IRS}^{sp(1)} + \mathbf{T}_{IRS}^{sp(1)\mathbf{T}}\mathbf{K}_{sp}^{(1)} + \mathbf{T}_{IRS}^{sp(1)\mathbf{T}}\mathbf{K}_{ss}^{(1)}\mathbf{T}_{IRS}^{sp(1)}$$

$$\mathbf{K}_{IRS}^{(12)} = \mathbf{K}_{pb}^{(1)} + \mathbf{K}_{ps}^{(1)}\mathbf{T}_{IRS}^{sb(1)} + \mathbf{T}_{IRS}^{sp(1)\mathbf{T}}\mathbf{K}_{sb}^{(1)} + \mathbf{T}_{IRS}^{sp(1)\mathbf{T}}\mathbf{K}_{ss}^{(1)}\mathbf{T}_{IRS}^{sb(1)}$$

$$\mathbf{K}_{IRS}^{(22)} = \mathbf{T}_{IRS}^{sb(1)\mathbf{T}}\mathbf{K}_{sb}^{(1)} + \mathbf{T}_{IRS}^{sb(1)\mathbf{T}}\mathbf{K}_{ss}^{(1)}\mathbf{T}_{IRS}^{sb(1)} + \mathbf{K}_{bs}^{(1)}\mathbf{T}_{IRS}^{sb(1)\mathbf{T}} + \mathbf{Kg}_{ii}^{(1)} + \mathbf{g}_{ib}^{(1)\mathbf{T}}\mathbf{G}^{(1)} + \mathbf{G}^{(1)\mathbf{T}}\left(\mathbf{g}_{bi}^{(1)} + \mathbf{g}_{bb}\mathbf{G}^{(1)}\right)$$

$$\mathbf{K}_{IRS}^{(23)} = \mathbf{g}_{ib}^{(1)\mathbf{T}}\mathbf{G}^{(2)} + \mathbf{G}^{(1)\mathbf{T}}\left(\mathbf{g}_{bj}^{(2)} + \mathbf{g}_{bb}\mathbf{G}^{(2)}\right)$$

$$\mathbf{K}_{IRS}^{(32)} = \mathbf{g}_{jb}^{(2)\mathbf{T}}\mathbf{G}^{(1)} + \mathbf{G}^{(2)\mathbf{T}}\left(\mathbf{g}_{bi}^{(1)} + \mathbf{g}_{bb}\mathbf{G}^{(1)}\right)$$

$$\mathbf{K}_{IRS}^{(22)} = \mathbf{T}_{IRS}^{sb(2)\mathbf{T}}\mathbf{K}_{sb}^{(2)} + \mathbf{T}_{IRS}^{sb(2)\mathbf{T}}\mathbf{K}_{ss}^{(2)}\mathbf{T}_{IRS}^{sb(2)} + \mathbf{K}_{bs}^{(2)}\mathbf{T}_{IRS}^{sb(2)\mathbf{T}} + \mathbf{Kg}_{jj}^{(2)} + \mathbf{g}_{jb}^{(2)\mathbf{T}}\mathbf{G}^{(2)} + \mathbf{G}^{(2)\mathbf{T}}\left(\mathbf{g}_{bj}^{(2)} + \mathbf{g}_{bb}\mathbf{G}^{(2)}\right) \tag{19}$$

$$\mathbf{M}_{IRS}^{(11)} = \mathbf{M}_{pp}^{(1)} + \mathbf{M}_{ps}^{(1)}\mathbf{T}_{IRS}^{sp(1)} + \mathbf{T}_{IRS}^{sp(1)\mathbf{T}}\mathbf{M}_{sp}^{(1)} + \mathbf{T}_{IRS}^{sp(1)\mathbf{T}}\mathbf{M}_{ss}^{(1)}\mathbf{T}_{IRS}^{sp(1)}$$

$$\mathbf{M}_{IRS}^{(12)} = \mathbf{M}_{pb}^{(1)} + \mathbf{M}_{ps}^{(1)}\mathbf{T}_{IRS}^{sb(1)} + \mathbf{T}_{IRS}^{sp(1)\mathbf{T}}\mathbf{M}_{sb}^{(1)} + \mathbf{T}_{IRS}^{sp(1)\mathbf{T}}\mathbf{M}_{ss}^{(1)}\mathbf{T}_{IRS}^{sb(1)}$$

$$\mathbf{M}_{IRS}^{(22)} = \mathbf{M}_{bb}^{(1)} + \mathbf{M}_{bs}^{(1)}\mathbf{T}_{IRS}^{sb(1)} + \mathbf{T}_{IRS}^{sb(1)\mathbf{T}}\mathbf{M}_{sb}^{(1)} + \mathbf{T}_{IRS}^{sb(1)\mathbf{T}}\mathbf{M}_{ss}^{(1)}\mathbf{T}_{IRS}^{sb(1)}$$

$$
\begin{aligned}
&+\mathbf{M}_{bb}^{(2)}+\mathbf{M}_{bs}^{(2)}\mathbf{T}_{IRS}^{sb(2)}+\mathbf{T}_{IRS}^{sb(2)\mathbf{T}}\mathbf{M}_{sb}^{(2)}+\mathbf{T}_{IRS}^{sb(2)\mathbf{T}}\mathbf{M}_{ss}^{(2)}\mathbf{T}_{IRS}^{sb(2)}\\
\mathbf{M}_{IRS}^{(23)}&=\mathbf{M}_{bp}^{(2)}+\mathbf{M}_{bs}^{(2)}\mathbf{T}_{IRS}^{sp(2)}+\mathbf{T}_{IRS}^{sb(2)\mathbf{T}}\mathbf{M}_{sp}^{(2)}+\mathbf{T}_{IRS}^{sb(2)\mathbf{T}}\mathbf{M}_{ss}^{(2)}\mathbf{T}_{IRS}^{sp(2)}\\
\mathbf{M}_{IRS}^{(33)}&=\mathbf{M}_{pp}^{(2)}+\mathbf{M}_{ps}^{(2)}\mathbf{T}_{IRS}^{sp(2)}+\mathbf{T}_{IRS}^{sp(2)\mathbf{T}}\mathbf{M}_{sp}^{(2)}+\mathbf{T}_{IRS}^{sp(2)\mathbf{T}}\mathbf{M}_{ss}^{(2)}\mathbf{T}_{IRS}^{sp(2)}
\end{aligned}
\tag{20}
$$

3. Numerical examples

This section presents examples to illustrate the effectiveness and accuracy of the proposed method in systems with non-matched interfaces. The reduced system of each domain is constructed with PDOFs. In the examples of non-matched systems, DOFs of domain interface frame and virtual DOFs of virtual interface are included in the reduced system for assembling each domain.

In each domain, around 5% DOFs are selected as PDOFs. Then, considering the inclusion of the IDOFs of a matched system, the total number of PDOFs is about 7-9% of the total DOFs of the global system. But, in a non-matched system, the number of the selected PDOFs is a little larger than the matched system because the IDOFs of the virtual frame are independent of the connected domains. Then, the reduced system of the non-matched system has 9-11% DOFs compared to the DOFs of the global system. In numerical examples, the error estimation is carried out as given in Eq. (21). To perform an eigenvalue analysis, an assumed hybrid stress shell element with four nodes is used [15].

$$
e(\%)=\left|\frac{\lambda_{\text{Global system}}-\lambda_{\text{Reduced system}}}{\lambda_{\text{Global system}}}\right| \tag{21}
$$

3.1 Non-matched structure with eight sub-domain plates

Originally, this structure consisted of six sub-domains with the compatible interface mesh. Previously, PDOFs and IDOFs were selected from six sub-domains. After assembling these six domains, domain 7 and domain 8 are assembled by the interface 1 and interface 2, respectively. Before attaching the sub-domains 7 and 8, the PDOFs and IDOFs of domain 7 and domain 8 are selected. The total number of DOF is 5952 and the number of the selected DOFs (PDOFs and IDOFs) is 556. It is about 9% DOFs of global system. Fig. 3 shows the detailed configuration for attaching the non-matched domain in interface 1 and interface 2. A penalty scheme is employed to attach

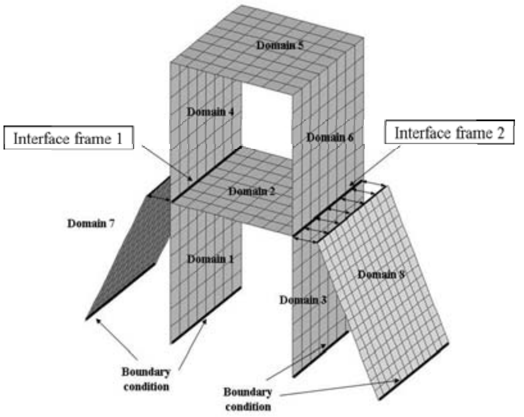

Fig. 3. Configuration of the arbitrary structure and partition of eight sub-domains.

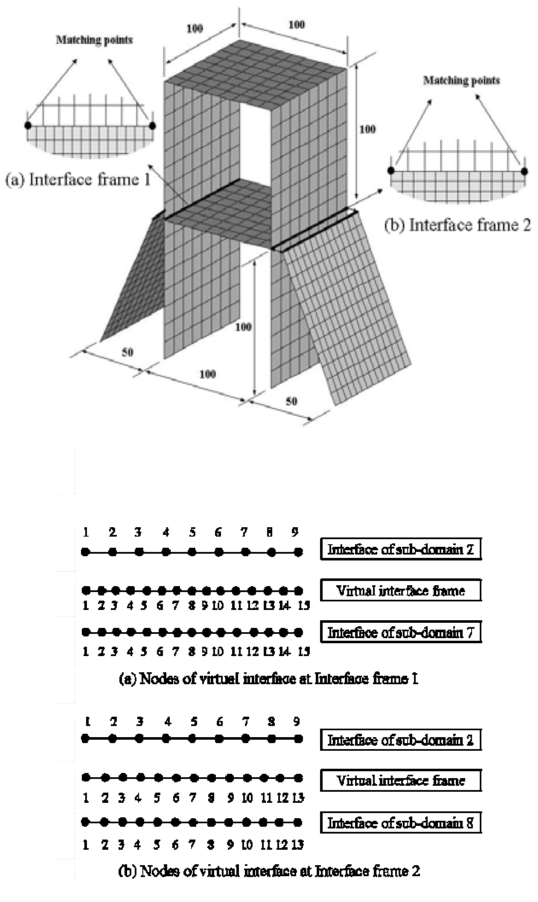

Fig. 4. Configuration of the interface frames and nodes of each interface frame.

each domain. The 15 virtual nodes (Fig. 4 (a)) and 13 virtual nodes (Fig. 4 (b)) are used for the virtual interface frames 1 and 2, respectively. The starting and ending points of the interface frame should be matched in each domain as shown in Fig. 4. For the interface frame, a linear interpolation function is employed in each element of the interface frame. The selection and a detailed description on how to choose the penalty value can be found in Pantano and Averill [7]

Fig. 5 is for the selection results of the candidate area and PDOFs in each domain from 1 to 8. In each domain, about 15-20% elements are selected as the candidate area. And 40 DOFs are selected as primary DOFs. When the sub-domains 7 and 8 are linked to the previous reduced system constructed with six domains, the changed reduced system is shown in Fig. 6. There is no need to arrange the node number or assemble each system. It is just required to make the size of the reduced system larger than the previous system considering the size of the additional systems.

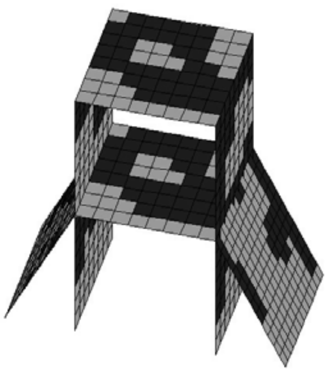

(a) Candidate area of six sub-domains

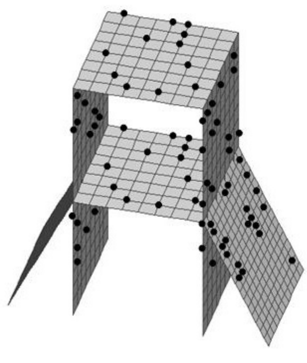

(b) Selected PDOFs of six sub-domains

Fig. 5. Selection of candidate area and selected DOFs for reduced system in eight sub-domains.

Table 1 shows the comparison result of the eigenvalue analysis between the global system and the reduced system. Maximum error value is just 0.7% at 20th eigenvalue. Moreover, IRS assures the reliability of the eigenvalue analysis in the ranges of not only the lower modes but also in the higher modes. The reduced system is well-constructed by the sub-domain scheme and it assures the reliability in various applications such as the time response of a dynamic problem or the design optimization based on the reduced system.

Table 1. Eigenvalue comparison of the global system and the reduced system(Ⅰ)

Mode No.	Global system (Hz)	Reduced system	
		Eigenvalue (Hz)	Error (%)
1	2.69	2.69	0.08
2	10.34	10.34	0.00
3	13.64	13.61	0.20
4	13.68	13.71	0.18
5	14.82	14.81	0.11
6	15.24	15.20	0.26
7	16.44	16.33	0.68
8	16.80	16.81	0.05
9	17.93	17.94	0.06
10	19.05	19.08	0.12
11	19.21	19.20	0.05
12	19.23	19.27	0.22
13	20.80	20.80	0.00
14	20.96	20.96	0.00
15	22.78	22.75	0.12
16	23.31	23.30	0.05
17	25.23	25.23	0.00
18	25.24	25.24	0.02
19	25.45	25.46	0.00
20	27.33	27.53	0.71

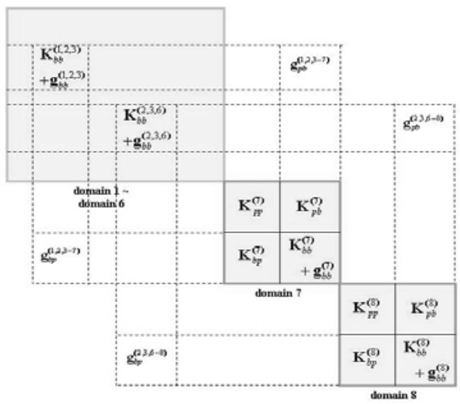

Fig. 6. Construction of the reduced system to assemble additional sub-systems.

3.2 Rear part of satellite projectile structure

The rear part of satellite projectile structure is given in Fig. 7 as a non-matched interface example. Sub-domain 1 consists of 480 elements and 481 node points. Four side fins with 256 elements and 289 nodes are attached to sub-domain 1. Fig. 7 shows the configuration of the attachment between the non-matched systems. In order to connect each system, the number of the interface frame elements of sub-domain 1 is 13 and the number of the interface elements of the domain 2,3,4, and 5 is 16. The element number in the virtual interface is 23.

Fig. 8 (a) and (b) show the selection of the candidate area and PDOFs in each domain. 80 elements from domain 1 and 40 elements from domains 1,2,3, and 4 are selected as the candidate area. 80 DOFs are selected as PDOFs in domain 1 and 30 DOFs are selected as PDOFs in domains 2,3,4, and 5. By in cluding the interface nodes, the total number of the selected DOFs is 920. It is about 9.34 % DOFs of the global system.

Table 2. Eigenvalue comparison of the global system and the reduced system(Ⅱ).

Mode No.	Global system(Hz)	Reduced system	
		Eigenvalue (Hz)	Error (%)
1	33.17	33.22	0.15
2	33.14	33.24	0.30
3	33.18	33.24	0.18
4	33.18	33.24	0.18
5	53.12	52.92	0.38
6	53.13	52.92	0.40
7	53.13	52.93	0.38
8	53.13	52.93	0.38
9	60.45	60.34	0.18
10	62.18	62.69	0.82
11	62.39	62.74	0.56
12	62.43	62.77	0.54
13	62.44	62.82	0.61
14	73.48	72.84	0.87
15	73.51	72.88	0.86
16	73.52	72.96	0.76
17	73.52	72.98	0.73
18	83.56	83.44	0.14
19	83.57	83.44	0.16
20	85.04	85.11	0.08

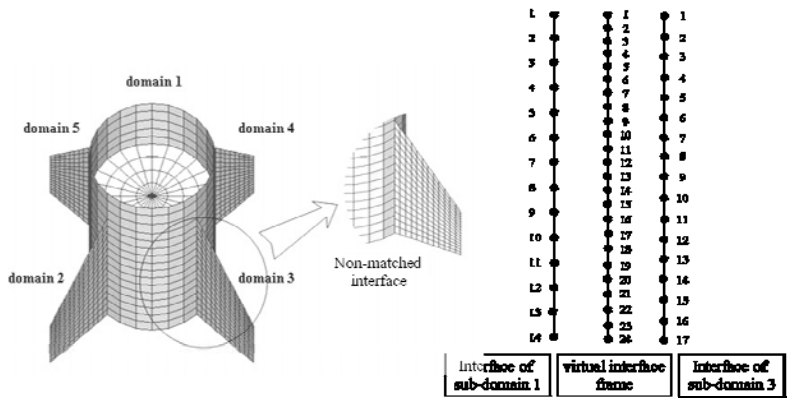

Fig. 7. Configuration of the rear part and five sub-domains of the satellite projectile model.

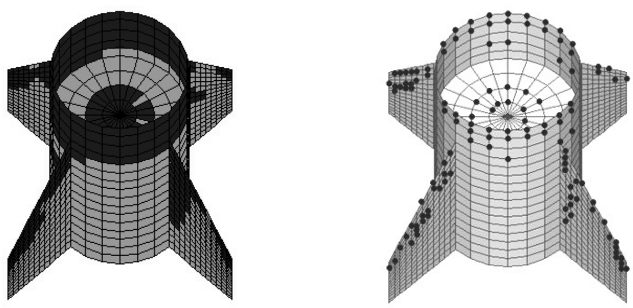

(a) Candidate area of each domain (b) Selected PDOFs of each domain

Fig. 8. Selection of candidate area and PDOFs of five sub-domains.

With a final reduced system of size [920×920], an eigenvalue analysis is performed and the results are given in Table 2. The maximum error is just 0.87% at the 14th mode. The present scheme, which has only one percent error in eigenvalue analysis, is adequate in structural analysis or structural optimization in engineering applications [16].

4. Conclusion

We have proposed a sub-domain scheme which assembles a reduced system based on PDOFs of each sub-domain in non-matched interface problems. The reduced system of each domain is constructed by TLCS. The employed scheme for the system condensation is an enhanced version in Cho and Kim [9]. But, the previous single domain reduction method is not suitable for large scale problems. The construction of the reduced system in the large-scale problem takes considerable time and requires a large amount of computer resources.

After partitioning the global system into several sub-domains, it is more efficient to construct the reduced system of each domain separately. In each sub-domain, DOFs are categorized into PDOFs, SDOFs and IDOFs. SDOFs are eliminated through the relation between SDOFs, PDOFs and IDOFs. After the selection of PDOFs, IRS is employed for the construction of the final reduced system. For the convenience of assembly of sub-domains, interface nodes between sub-domains are included in the reduced system. Once the PDOFs are properly selected from total active DOFs, IRS assures adequate accuracy compared to more refined and improved schemes such as subspace iteration method.

For verifying the reliability and the efficiency of the proposed scheme, two kinds of examples are presented. In non-matched systems, the interface connection between each sub-domain is performed by the penalty frame method.

In the structural optimization of dynamic problems, large-scaled problems require a large amount of computing time for dynamic analysis and sensitivity computations. The present study can be extended to the design sensitivity analysis. In order to enhance the efficiency of the proposed scheme, the present sub-domain reduction method will be extended to the sub-domain scheme which requires parallel-computation in the selection of PDOFs of each domain.

Acknowledgments

Authors are gratefully acknowledging the financial support by Defense Acquisition Program Administration and Agency for Defense Development under the contract UD070041AD.

References

[1] Jr. Craig and C. Bampton, Coupling of substructures for dynamic analyses, *AIAA Journal* 6 (7) (1968) 1313-1319.

[2] C. Farhat and F. X. Roux, A method of finite element tearing and interconnecting and its parallel solution algorithm, *Int. J. Numer. Mech. Engng.* 32 (1991) 1205-1228.

[3] A. Gravouil and A. Combescure, Multi-time step explicit-implicit method for non-linear structural dynamics, *Int. J. Numer. Mech. Engng.* 50 (1) (2001) 199-225.

[4] M. A. Aminpour, J. B. Ransom and S. L. Mccleary, A coupled analysis method for structures with independently modeled finite element subdomains, *Int. J. Numer. Mech. Engng.* 38 (21) (1995) 3695-3718.

[5] V. Faucher and A. Combescure, A time and space mortar method for coupling linear modal subdomains and non-linear subdomains inexplicit structural dynamics, *Comput. Methods Appl. Mech. Engrg.*192 (5-6) (2003) 509-533.

[6] M. Cho and W. B. A, Kim, Coupled finite element analysis of independently modeled substructures by penalty frame method, *KSME International Journal* 16 (10) (2002) 1201-1210.

[7] A. Pantano and R. C. Averill, A penalty-based finite element interface technology, Comput. Struct. 80 (22) (2002) 1725-1748.

[8] A. Pantano and R. C. Averill, A mesh-independent interface technology for simulation of mixed-mode delamination growth, *Int. J. Solids Struct*. 41 (14) (2004) 3809-3831.

[9] M. Cho and H. Kim, Element-based node selection method for reduction of eigenvalue problems, *AIAA Journal* 42 (8) (2004) 1677-1684.

[10] H. Kim and M. Cho, Construction of reduced system by two-level condensation scheme and refined sensitivity analysis, 45th AIAA/ASME/ASCE/AHS/ASC Structures, Structural Dynamics and Materials Conference, Palm Springs, California, (2004).

[11] H. Kim and M. Cho, Two-level scheme for selection of primary degrees of freedom and semi-

analytic sensitivity based on the reduced system, *Comput. Methods Appl. Engrg.*195 (33-36) (2006) 4244-4268.

[12] H. Kim and M. Cho, Improvement of reduction method combined with sub-domain scheme in large scale problem, *Int. J. Numer. Mech. Engng.* 70 (2) (2006) 206-251.

[13] R. J. Guyan, Reduction of stiffness and mass matrices, *AIAA Journal* 3 (2) 380.

[14] J. O'Callahan, A procedure for an improved reduced system (IRS) model, Proceedings of the 7th international modal analysis conference, Union college, Schenectady. NY, (1989).

[15] M. A. Aminpour, An assumed stress hybrid 4 node shell element with drilling degrees of freedom, *Int. J. Numer. Mech. Engng*. 33 (1) (1992) 19-38.

[16] M. Cho and H. Kim, Size and shape optimization combined with equivalent static loads in reduced system, 6th World Congress on Computational Mechanics (WCCM), Beijing, China, (2004).

[17] H. Kim and M. Cho, Dynamic analysis of reduced system partitioned by domain decomposition**,** 46th AIAA/ASME/ASCE/AHS/ASC Structures, Structural Dynamics and Materials Conference, Austin, Texas, (2005).